Can Remote Substituent Effects Influence Reactivity and Stereoselectivity in the Diels–Alder Cycloadditions of *p*-Substituted 6-Phenyl-6-methylfulvenes?

M. M. Gugelchuk,* P. C.-M. Chan, and T. J. Sprules

Department of Chemistry, University of Waterloo, Waterloo, Ontario, Canada N2L 3G1

Received July 22, 1994[⊗]

The kinetics, activation parameters, and stereoselectivity in the Diels–Alder reaction of a series of *p*-substituted 6-phenyl-6-methylfulvenes with *N*-phenylmaleimide have been measured in benzene-d_6 to examine the consequence of remote electronic perturbation on the system. The variation in equilibrium endo:exo ratios as a function of substituent adheres very well to a LFER with σ^+ ($\varrho = 0.701$) in contrast to the kinetic stereoselectivity which shows no linear relationship of the Hammett type. A reasonably good LFER with σ^- is observed for the reactivities, especially when the NMe_2 and OMe examples are excluded ($\varrho = -0.684$). Temperature and solvent effects on these properties have also been investigated. Substituent-induced changes in preferred conformation and π-electron densities of the fulvenes have been studied by *ab initio* molecular orbital calculations. The optimum twist angle between the π-subsystems remained relatively constant (54–55°) across the series except in the case of *p*-NMe_2 substitution where it is substantially decreased (36°). Relative reactivities and kinetic stereoselectivities are seen to have a connection with the calculated magnitude and direction of the fulvene molecular dipole moment. The importance of frontier MO energies was examined.

Introduction

Renewed interest in substituent effects on 6-arylfulvenes has arisen due to their potential as organic nonlinear optical materials.[1] It has been suggested that the charge transfer interaction resulting from aromaticities of these nonbenzenoid aromatics can be as effective in producing nonlinear optical responses as that from electronegativities in heteroatoms, especially when Z is a strong donor substituent (Scheme 1).[1b] On the other hand, for 6-arylfulvenes in which Z is a strong acceptor substituent, charge transfer in the opposite sense (Scheme 2) could cause these fulvenes to exhibit antiaromatic properties.[2] This polar contribution is thought to be greater in the excited state, and assuming they have a low-lying triplet excited state, antiaromatic fulvenes could be promising as charge-transfer organic ferromagnetic materials.[3] The high polarizability of 6-arylfulvenes has been documented experimentally by dipole moment evaluations,[4] electronic absorption spectroscopy,[5] and ^1H NMR and ^{13}C NMR spectroscopy[6] and theoretically by various molecular orbital studies.[1a,5,6a,7]

As part of a larger study on the transmission of substituent effects through extended π-systems, this paper reports a systematic examination of long-range electronic perturbation on rate and stereochemistry for the [4 + 2] cycloaddition of a series of *p*-substituted phenylfulvenes with *N*-phenylmaleimide along with related molecular orbital calculations in an attempt to assess the importance of dipolar resonance forms to the observed behavior of the molecule. Although the theory of substituent effects on nonalternant π-systems is less well-developed than that of alternant systems, employing Diels–Alder cycloadditions to test electronic theory and reactivity in this class of compounds allows one to make use of the wealth of data regarding substituent effects on these pericyclic reactions. We are also interested in examining the possibility of long-range electronic modulation of endo/exo stereoselectivity in this system. Relevant to this issue is a recent assessment of substituent

Scheme 1

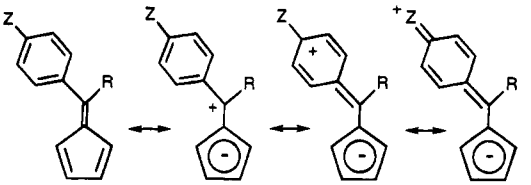

Scheme 2

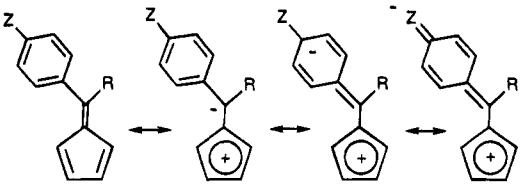

[⊗] Abstract published in *Advance ACS Abstracts,* November 15, 1994.

(1) (a) Wingert, L. M.; Staley, S. W. *Acta Crystallogr.* **1992**, *B48*, 782–789. (b) Papadopoulos, M. G.; Waite, J. *J. Chem. Soc., Faraday Trans.* **1990**, *86*, 3525–3529. (c) Ikeda, H.; Kawabe, Y.; Sakai, T.; Kawasaki, K. *Chem. Phys. Lett.* **1989**, *157*, 576–578. (d) Kawabe, Y.; Ikeda, H.; Sakai, T.; Kawasaki, K. *J. Mater. Chem.* **1992**, *2*, 1025–1031.

(2) Chandrasekhar, S.; Venkatesan, V. *J. Chem. Research, Miniprint* **1989**, 2056–2076.

(3) LePage, T. J.; Breslow, R. *J. Am. Chem. Soc.* **1987**, *109*, 6412–6421.

(4) (a) Kresze, G.; Goetz, H. *Chem. Ber.* **1957**, *90*, 2161–2176. (b) Kresze, G.; Rau, S.; Sabelus, G.; Goetz, H. *Liebigs Ann. Chem.* **1961**, *648*, 57–63.

(5) Griffiths, J.; Lockwood, M. *J. Chem. Soc., Perkin Trans. 1* **1976**, 48–53.

(6) (a) Sardella, D. J.; Keane, C. M.; Lemonias, P. *J. Am. Chem. Soc.* **1984**, *106*, 4962–4966. (b) Boenzli, P.; Otter, A.; Neuenschwander, M.; Huber, H.; Kellerhals, H. P. *Helv. Chim. Acta* **1986**, *69*, 1052–1064. (c) Otter, A.; Muehle, H.; Neuenschwander, M.; Kellerhals, H. P. *Helv. Chim. Acta* **1979**, *62*, 1626–1631. (d) Pines, A.; Rabinovitz, M. *J. Chem. Soc. B* **1971**, 385–388.

(7) (a) Takeno, N.; Takano, N.; Morita, M. *Nippon Kagaku Kaishi* **1972**, 983–985. (b) Houk, K. N.; George, J. K.; Duke, R. E., Jr. *Tetrahedron* **1974**, *30*, 523–533. (c) Fox, M. A.; Cardona, R.; Kiwiet, N. J. *J. Org. Chem.* **1987**, *52*, 1469–1474. (d) Fabian, W. M. F. *J. Comput. Chem.* **1988**, *9*, 369–377.

0022-3263/94/1959-7723$04.50/0

Scheme 3

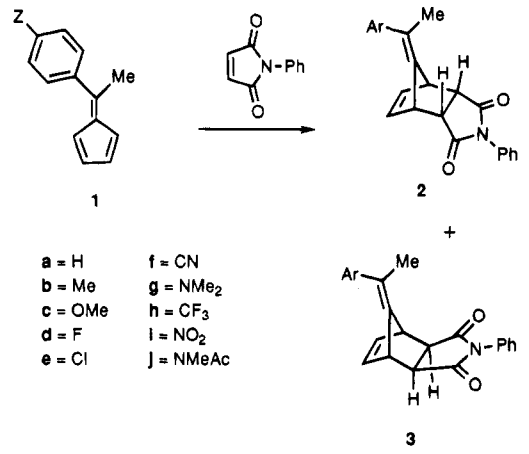

effects that demonstrated remote electronic influences can directly affect π-facial stereoselection in Diels-Alder cycloadditions of related fulvenes with certain dienophiles.[8]

Results and Discussion

Diels–Alder Reaction with *N*-Phenylmaleimide. To analyze the substituent electronic effects, variations were selected to broadly represent a sufficient range of inductive and resonance interactions. When heated to 30–80 °C with *N*-phenylmaleimide in benzene-d_6, all fulvenes **1** proceeded to give a mixture of adducts, **2** and **3**, with the predominant isomer arising from endo addition (Scheme 3).

These isomers exhibit individually characteristic ^{1}H NMR spectra. The most diagnostic signals to distinguish the endo and exo adducts are those due to the α-carbonyl protons. In the endo adduct, these protons are exo on the norbornene ring and couple to the adjacent bridgehead protons. Their signal in $CDCl_3$ appears as a doublet of doublets at δ 3.4–3.5. In the exo adduct these protons are endo on the norbornene ring, and due to the near 90° dihedral angle between them they do not effectively couple to the adjacent bridgehead protons. Instead, their signal appears as a doublet at higher field around δ 2.9–3.0. The higher field shift ($\Delta\delta$ = 0.2) in the exo isomer is expected as a result of the anisotropy of the endocyclic double bond.

An anisotropic effect of the aryl ring on the exocyclic double bond is observed in the chemical shift of the bridgehead protons. For both isomers, the bridgehead proton nearest the aryl ring is deshielded by 0.2 ppm compared to its counterpart anti to the ring. These proton resonances occur at δ 3.9 and 4.1 in the endo adducts and at δ 3.8 and 4.0 in the exo adducts. For a given isomer, the chemical shifts across the series showed no dependence on the nature of the para substituent except for those protons directly on the aryl ring. Full characterizations can be found in the supplementary material.

Kinetic Data for Cycloaddition. Even upon storage in the freezer, the fulvenes (except **1c** and **1g**) have a tendency to dimerize. The fulvenes were purified immediately before use in the kinetic studies. In many cases, the monomer could be regenerated cleanly from the dimer by moderate heating. The kinetic runs were studied in benzene at 80 °C and followed to 83–95% completion by ^{1}H NMR analysis of the disappearing fulvene **1** and the appearing cycloadducts **2** and **3** (see Experimental Section for details). An equimolar amount of reactants was used and the reactions all showed clean second-order kinetics over *ca.* 5 half-lives. The second-order rate constants given in Table 1 were determined by linear least-squares regression of a plot of 1/[fulvene] versus time. Close scrutiny of the NMR data for signals due to fulvene dimers indicated this possible side-reaction was not competitive under the conditions. The only fulvene showing traces of dimerization during the kinetic runs was **1h** (Z = CF_3).

Table 1. Reactivity[a] and Stereoselectivity[b] Data

Z	10^2k_{obs}	N/X[c]	N/X[d]
NMe_2	3.61 ± 0.2	7.7 ± 0.5	1.0 ± 0.0
OMe	3.66 ± 0.4	9.3 ± 0.8	2.2 ± 0.2
F	5.34 ± 0.5	7.5 ± 0.7	3.6 ± 0.3
Cl	4.59 ± 0.3	8.8 ± 0.3	4.1 ± 0.4
Me	5.24 ± 0.3	10.6 ± 0.7	3.0 ± 0.4
CF_3	4.35 ± 0.4	12.2 ± 0.2	5.5 ± 0.4
CN	2.21 ± 0.1	10.1 ± 0.2	5.0 ± 0.3
NO_2	2.59 ± 0.1	10.5 ± 0.5	5.6 ± 0.1
H	6.28 ± 0.8	9.6 ± 0.7	3.0 ± 0.3
NMeAc	1.86 ± 0.2	6.7 ± 0.4	3.2 ± 0.2

[a] Second-order rate constants (in L/mol s) and endo/exo ratios were obtained from the averages of multiple kinetic runs over 30 min at 80 °C in C_6D_6. $[fulvene]_o = [maleimide]_o$ = 0.0667 M. [b] Standard deviations of the averages. [c] Kinetic endo:exo ratios (N/X) at 80 °C. [d] Equilibrium endo:exo ratios (N/X) obtained after extended reaction times (≥96 h) at 80 °C.

Diels–Alder cycloadditions of many fulvenes are known to be reversible.[9] To demonstrate that the observed stereoselection at short reaction times is a result of kinetically-controlled dienophile capture, the individual adducts were subjected to the reaction conditions and the sample monitored at 5 min intervals by ^{1}H NMR for the appearance of the other isomer. No isomerization was observed at temperatures of 30–80 °C over a time span of 1 h. Replacement of hydrogen by any substituent resulted in a decrease in the rate of reaction. This is consistent with a previous study on the kinetics of a few *p*-substituted diphenylfulvenes with maleic anhydride (k_{rel}: H > Me > OMe > Cl).[9a]

We also monitored the reaction over extended times up to 120 h at 80 °C. Only after 5 h did the endo/exo ratios (N/X) begin to change slowly up to 96 h after which the reaction had reached equilibrium (see Table 1). The observed substituent influence can be summarized as follows:

reactivity: H > F, Me > Cl, CF_3 > OMe, NMe_2 > NO_2, CN

Kinetic Endo Selectivity: CF_3 > Me, NO_2 > CN, H > OMe > Cl > NMe_2, F

Thermodynamic Endo Selectivity: NO_2, CF_3 > CN > Cl > F > Me, H > OMe > NMe_2

(8) (a) Gugelchuk, M.; Paquette, L. A. *J. Am. Chem. Soc.* **1991**, *113*, 246–253. (b) Gugelchuk, M.; Paquette, L. A. *Isr. J. Chem.* **1989**, *29*, 165–169. (c) Paquette, L. A.; Gugelchuk, M. *J. Org. Chem.* **1988**, *53*, 1835–1837.

(9) (a) Konovalov, A. I.; Yarkova, E. G.; Salikhov, I. Sh.; Izmailova, R. G. *Zh. Org. Khim.* **1967**, *3*, 1319–1323. (b) Hughes, M. T.; Williams, R. O. *J. Chem. Soc., Chem. Commun.* **1978**, 587–588. (c) Onishchenko, A. S. *Diene Synthesis*; Israel Program for Scientific Translations: Jerusalem, 1964. (d) Yates, P. *Advances in Alicyclic Chemistry*; Hart, H., Karabatsos, G. J., Eds.; Academic Press: New York, 1968; Vol. 2, pp 20–184.

Indeed, the results provide evidence for long-range substituent effects on the rate of reaction and the stereoselectivity. The kinetic endo preference is understandable in terms of steric interactions and the usual secondary orbital overlap stabilization. Of note, the degree of kinetic endo selectivity does not have a simple relationship to the observed reactivity nor to the electronic nature of the substituent. There is, however, a discernible trend with electronic character seen in the order of thermodynamic stabilities of the cycloadducts. Presumably the exo adduct is the more stable species since in all examples there was an increased proportion of the exo adduct in the equilibrium mixture. The data show that as the donor ability of the para substituent increases, the amount of exo adduct at equilibrium also increases.

A possible explanation is that strong donor groups could stabilize the transition state for retro-Diels–Alder dissociation through enhanced contributions from resonance structures containing aromatized fulvene rings. On this basis, the cycloadducts from **1g** would be expected to have the lowest activation energy for the isomerization pathway. This idea was supported by the results of **1j** where one methyl group is replaced by an acetyl group. Delocalization of the nitrogen lone pair into the carbonyl would curtail its ability to donate into the phenyl ring, and it was seen that the equilibrium composition of **1j** was similar to that of **1a** and **1b**.

To address the question of whether stereoselectivity in this class of compounds may be dienophile dependent, we individually reacted **1g** (Z = NMe_2) and **1f** (Z = CN) with maleic anhydride at 70 °C in C_6D_6. In both cases, a 1:1 mixture of endo:exo adducts was observed after 1 h (70–80% completion) which suggests the *N*-phenyl substituent may play a role in stereoselectivity.

In an attempt to better understand the observed substituent effects, we performed a statistical evaluation of the data by means of three methods: simple Hammett,[10] dual substituent parameter (DSP),[11] and Taft–Topsom multiparameter analyses.[12] The Taft–Topsom treatment is a generalized substituent effect theory involving four primary substituent effects: electronegativity (χ), polarizability (α), field (F), and resonance (R). Consideration of the number of degrees of freedom was taken into account by examining the Exner ψ statistic.[13] Using this standard, the lower the value of ψ, the better the fit (0.5 being the utmost acceptable limit). Unconstrained correlations (e.g., the property correlated is not expressed relative to H as substituent) were carried out to allow a check of the intercept term for effects connected with replacement of hydrogen by any other substituent. For multiparameter analyses, the relative importance of the various influences was measured by a weighted assessment of the regression coefficients.[14]

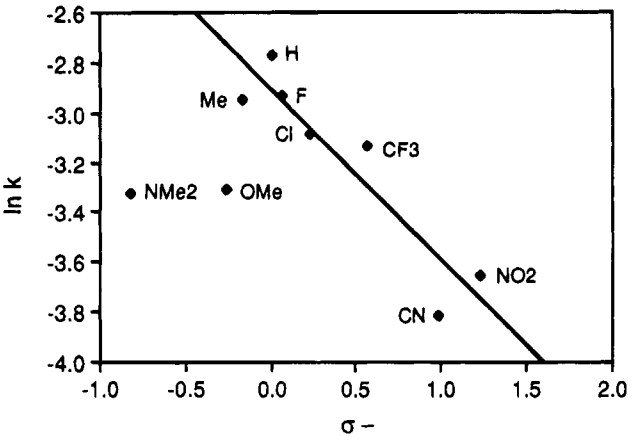

Figure 1. Hammett plot of 2nd-order rate constants versus σ^-. The straight line represents the least-squares regression fit omitting NMe_2 and OMe points: $\ln k = -2.907 - 0.6840\sigma^-$, standard error of estimate = 0.161.

Statistical Analysis of Substituent Effect on Rate (80 °C, C_6D_6). A simple Hammett analysis gave poor correlation between ln *k* and all the substituent constants σ_p, σ^+, or σ^-. The best fit was obtained using σ^- (r = 0.55, ψ = 0.95). Examination of the Hammett plot (Figure 1) indicates the NMe_2 and OMe substituents are much less reactive than expected from their substituent constants. Their maverick reactivities can be rationalized on the basis that the two strongest donor substituents would have the largest contribution of resonance structures having an aromatic five-membered ring. This would presumably stabilize the reactant more than the TS and thus decrease the expected rate of reaction. Exclusion of the NMe_2 and OMe data points gave greatly improved correlations with the best fit being between ln *k* and σ^- (ϱ = −0.684, r = 0.93, ψ = 0.4). Small reaction constants are typical for concerted reactions and the decrease in reactivity with increasing electron accepting character of the substituent is as expected for a normal electron demand Diels–Alder reaction. The best correlation occurring with σ^- parameters but having a negative slope usually implies a situation where electron withdrawal stabilizes the reactant more than the corresponding transition state. Of the substituents included in the analysis, only the strong acceptor substituents (e.g., CN and NO_2) would give rise to an additional contributing resonance structure involving charge transfer directly to the substituent. The Hammett plot could be rationalized assuming this would be more favorable in the fulvene than the Diels–Alder transition state.

Using the DSP method, no good correlation was found between ln *k* and any pair of σ_I, σ_R parameters when all data points were included. The best fit was obtained using σ_I, σ_R^- (r = 0.67, ψ = 0.90). Exclusion of the NMe_2 and OMe data points provided an improved correlation between ln *k* and σ_I, σ_R^- (r = 0.92, ψ = 0.5). Least-squares regression gave $\ln k = -2.90 - 0.726\sigma_I - 0.765\sigma_R^-$, standard error of estimate = 0.191. Resonance effects (57.3%) are predicted to be slightly more important than inductive effects (42.7%) in determining reactivity. However, the incorporation of a second substituent parameter (σ_I) into the analysis decreases the goodness of fit and, furthermore, yields no improvement in explaining the variation in the series any better than the one-term LFER (*vide supra*).

The Taft–Topsom method demonstrated a fair correlation between ln *k* and the set of σ_χ, σ_α, σ_R substituent

(10) (a) McDaniel, D. H.; Brown, H. C. *J. Org. Chem.* **1958**, *23*, 420–427. (b) Hoefnagel, A. J.; Monshouwer, J. C.; Snorn, E. C. G.; Wepster, B. M. *J. Am. Chem. Soc.* **1973**, *95*, 5357–5366. (c) Liotta, C. L.; Smith, D. F., Jr.; Hopkins, H. P., Jr.; Rhodes, K. A. *J. Phys. Chem.* **1972**, *76*, 1909–1912.

(11) (a) Topsom, R. D. *Prog. Phys. Org. Chem.* **1976**, *12*, 1–20. (b) Ehrenson, S.; Brownlee, R. T. C.; Taft, R. W. *Prog. Phys. Org. Chem.* **1973**, *10*, 1–79.

(12) Taft, R. W.; Topsom, R. D. *Prog. Phys. Org. Chem.* **1987**, *16*, 1–83.

(13) Shorter, J. *Correlation Analysis of Organic Reactivity*; Wiley: New York, 1982; Chapter 7.

(14) Weighted assessments were used to avoid misleading impressions of relative importance due to the different numerical scales of the substituent constants. Each regression coefficient was weighted by the standard deviation of the corresponding independent variable (i.e., weighting factor = $[\Sigma(\sigma - \bar{\sigma})^2/n - 1]^{1/2}$).

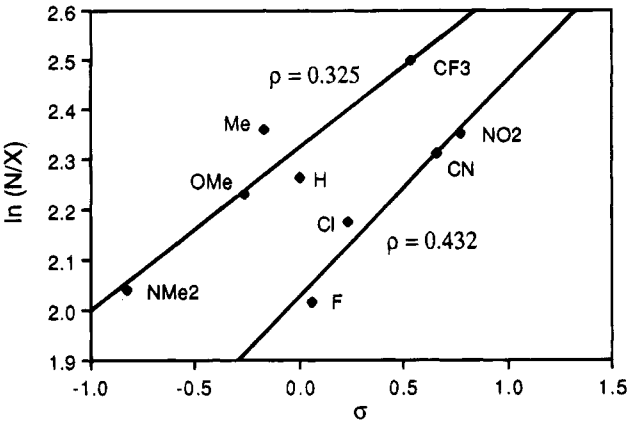

Figure 2. Hammett plot of kinetic endo selectivity at 80 °C versus σ. The straight lines represent the least-squares regression fits.

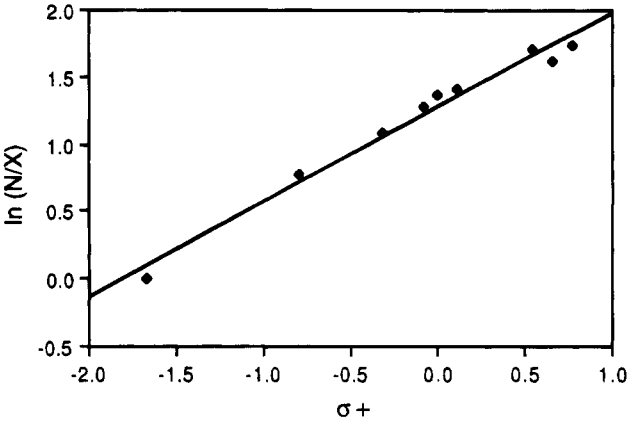

Figure 3. Hammett plot of equilibrium endo selectivity at 80 °C versus σ^+. The straight line represents the least-squares regression fit: ln (N/X) = 1.276 + 0.701σ^+; standard error of estimate = 0.089.

constants (r = 0.92, ψ = 0.5). Least-squares regression gave ln k = −2.649 − 1.090σ_χ + 1.416σ_α − 0.660σ_R, standard error of estimate = 0.172. This model predicts a combination of 37.5% electronegativity, 38.9% polarizability, and 23.6% resonance effects comprising the overall substituent effect. Exclusion of the NMe_2 and OMe data points strengthened the correlation between ln k and the set of σ_χ, σ_α, σ_R substituent constants (r = 0.98, ψ = 0.2). Least-squares regression gave ln k = −2.735 − 0.997σ_χ + 1.098σ_α − 1.504σ_R, standard error of estimate = 0.098. Omission of these points caused only slight quantitative changes in the relative importance of effects (34.0% electronegativity, 36.7% polarizability and 29.3% resonance). Of note, this model contradicts the previous expectation of a predominant resonance component to explain reactivity in the series.

Statistical Analysis of Substituent Effect on Kinetic Stereoselectivity (80 °C, C_6D_6). Poor correlation was found between ln (N/X) and all the substituent constants σ_p, σ^+, or σ^- (r = 0.57−0.62). Examination of the Hammett plot (Figure 2) suggests there could be two different correlation lines for stereoselectivity, one with NMe_2, OMe, Me, H, and CF_3 substituents (r = 0.94) and another with F, Cl, CN, and NO_2 substituents (r = 0.97). Alternatively, there may be no linear relationship between the kinetic endo/exo selectivity and Hammett substituent constants. This is not surprising when one considers that the measured substituent effect reflects not only the nature of the substituent group but also its ability to respond to the electronic and structural changes produced in going from reactants to transition state, as well as differences in solvation. A LFER would exist only if the composition of the electronic effect of substituents in this system is comparable to that of the substituent constants used.

DSP analysis gave better, but still poor, correlation between ln (N/X) and all pairs of σ_I, σ_R. The best fit was obtained using either σ_I, σ_R° (R = 0.80, ψ = 0.7) or σ_I, $\sigma_{R(BA)}$ (r = 0.80, y = 0.7) with all data points included. Least-squares regression gave ln (N/X) = 2.364 − 0.121σ_I + 0.525σ_R°, standard error of estimate = 0.108. The relative importance of influences from this model is 81.0% resonance to 19.0% inductive effects.

A comparable correlation was obtained by a Taft−Topsom analysis. The best correlation was between ln (N/X) and the set of σ_χ, σ_R substituent constants (r = 0.82, ψ = 0.7). Least squares regression gave ln (N/X) = 2.361 − 0.225σ_χ + 0.356σ_R, standard error of estimate = 0.104. A considerable contribution of resonance effects (62.3%) relative to electronegativity effects (37.7%) is indicated by the weighted assessment of this model. There was no significant improvement in correlation by the inclusion of additional explanatory variables. Incorporation of σ_α gave an improvement in r of only 0.01 and would explain only 6% of the remaining variation in ln (N/X). It also led to a slight increase in the standard deviations of the regression coefficients, ϱ_χ and ϱ_R. The lack of a good correlation with any of the above methods signals the importance of other factors, possibly steric ones, on the kinetic stereoselectivity.

Statistical Analysis of Substituent Effect on Equilibrium Stereochemistry (80 °C, C_6D_6). Excellent correlation (ϱ = 0.701, r = 0.99, ψ = 0.17) was found between ln (N/X) and σ^+ with all data points included (Figure 3). Poorer correlations were obtained with σ_p (r = 0.95, ψ = 0.36) or σ^- (r = 0.88, ψ = 0.53). The best correlation occurring with σ^+ parameters supports the view that strong donor groups could stabilize the transition state for retro-Diels−Alder dissociation through enhanced contributions from resonance structures containing aromatized fulvene rings. Using the DSP method, excellent correlation was found between ln (N/X) and σ_I, σ_R^+ (r = 0.99, ψ = 0.18). Least-squares regression gave ln (N/X) = 1.327 + 0.562σ_I + 0.734σ_R^+, standard error of estimate = 0.092. This model is composed of 76.2% resonance to 23.8% inductive effects. Poorer correlations were obtained by Taft−Topsom analyses. The best fit was between ln (N/X) and the set of σ_χ, σ_R substituent constants (r = 0.82, ψ = 0.7). Least-squares regression gave ln (N/X) = 2.361 − 0.225σ_χ + 0.356σ_R, standard error of estimate = 0.104. A blend of 62.3% resonance to 37.7% electronegativity effects is predicted. All three methods predict a large influence on equilibrium stereoselectivity by resonance effects.

Temperature Effects. We investigated the influence of temperature on the reactivity and stereoselectivity of selected fulvenes (**1a**, **1f**, and **1g**) to examine the substituent effect on the corresponding activation parameters. These fulvenes were chosen as representative examples for neutral, strong acceptor and strong donor substituents. The results are summarized in Table 2. Analysis of the Arrhenius and Eyring plots provided the activation parameters that appear in Table 3. By assuming the kinetic endo:exo product ratio (N/X) is equal to the ratio of the rate constants (k_N/k_X), the differences

Table 2. Temperature Effects on Reactivity[a] and Stereoselectivity[b]

T (°C)	10^3k_{obs} (H)	N/X (H)	10^3k_{obs} (NMe_2)	N/X (NMe_2)	10^3k_{obs} (CN)	N/X (CN)
30	1.51 ± 0.1	≥19.0[d]	1.24 ± 0.0	15.7 ± 0.1	0.88 ± 0.0	≥19.0[d]
40	4.51 ± 0.1	≥19.0[d]	3.30 ± 0.3	9.8 ± 0.7	1.98 ± 0.1	18.2 ± 0.6
50	8.16 ± 0.3	≥19.0[d]	7.47 ± 0.5	9.1 ± 1.2	3.81 ± 0.1	11.8 ± 0.8
60	17.0 ± 1.0	15.4 ± 0.3	12.7 ± 0.3	8.7 ± 0.6	7.92 ± 0.2	12.7 ± 0.5
70	35.3 ± 2.0[c]	11.2 ± 1.4	17.8 ± 0.8	7.5 ± 1.1	14.2 ± 0.3	11.3 ± 0.2
80	62.8 ± 8.0	9.6 ± 0.7	36.1 ± 2.0	7.7 ± 0.5	22.1 ± 0.9	10.1 ± 0.2

[a] Second-order rate constants (L/mol s) and endo/exo ratios obtained from kinetic runs over 30 min in C_6D_6. $[fulvene]_o = [maleimide]_o = 0.0667$ M. Standard error of the rate constant from least-squares regression. [b] Standard deviation is given for the average of the ratio over the course of the kinetic run. [c] Over a 20 min kinetic run. [d] Actual concentration of exo adduct could not be determined due to signal-to-noise ratio complications when present at ≤5%.

Table 3. Arrhenius and Eyring Activation Parameters[a]

Z	E_a	A	$\Delta H^{\ddagger}$	$\Delta S^{\ddagger}$	$\Delta\Delta H^{\ddagger,b}$	$\Delta\Delta S^{\ddagger,b}$
H	15.5	251×10^6	14.9	−22.3	5.5	−11.2
CN	13.8	8.12×10^6	13.2	−29.0	2.7	−3.9
NMe_2	13.6	10.1×10^6	13.0	−28.7	2.7	−3.8

[a] Energies are given in kcal/mol. Entropies are given in cal/mol K. Arrhenius A factors are given in L/mol s. The estimated uncertainty is ±1 kcal/mol in energy terms and ±2 eu in entropy terms. [b] The values given were determined from the intercepts and slopes of plots of ln (k_N/k_X) vs $1/T$ using the equations $\Delta\Delta H^{\ddagger} = \Delta H^{\ddagger}_X - \Delta H^{\ddagger}_N = E_a(X) - E_a(N)$ and $\Delta\Delta S^{\ddagger} = \Delta S^{\ddagger}_N - \Delta S^{\ddagger}_X = R \ln (A_N/A_X)$.

in activation parameters for endo and exo addition were obtained by plots of ln (k_N/k_X) vs $1/T$.

The relatively small enthalpies of activation and the large negative entropies of activation are typical of concerted Diels–Alder reactions. A compensatory effect exerted on the activation parameters is suggested by the data. Whether the para substituent is a strong donor or strong acceptor, the change from hydrogen appears to cause a stronger interaction between reactants (decreasing $\Delta H^{\ddagger}$) accompanied by tighter binding in the transition state (more negative $\Delta S^{\ddagger}$) in comparison to the unsubstituted case. Concerning the differences in endo/exo activation parameters, entropy changes are more favorable in the exo TS concomitant with less favorable enthalpy changes compared to the endo TS.

Solvent Effects. The influence of solvent was briefly investigated to determine the response of the stereoselectivity to a change in solvent polarity. If this was important, the differences in polarization of the endo and exo transition states may be susceptible to modulation by electrostatic interactions with solvent. The more polar transition state would be more greatly affected by increasing the dielectric constant of the solvent and therefore we might see a substituent dependent variation in stereoselectivity with an increase in solvent polarity.

As expected for a concerted Diels–Alder mechanism, solvent effects on reactivity were small, yet there is a marked difference in the response of **1f** (Z = CN) and **1g** (Z = NMe_2) to a change in solvent polarity (Table 4). The rate of reaction of **1f** was seen to slightly increase as did the stereoselectivity with increasing dielectric constant. There was no effect on the stereoselectivity of **1g** within the limits of experimental error, however the reaction was *ca.* twice as slow in acetone as in benzene or DMSO. A plot of ln k versus the Kirkwood function is linear for **1f** but is widely scattered for **1g** (Figure 4) which may indicate nonelectrostatic or specific solvent–solute interactions are involved in the latter case. Although more detailed studies are needed to properly analyze the electrostatic interactions, the results suggest the Diels–Alder transition state of **1f** has more development of charge than that of **1g**.

Table 4. Solvent Effects on Reactivity[a] and Stereoselectivity[b]

parameter	benzene-d_6 $\epsilon = 2.3$	acetone-d_6 $\epsilon = 20.7$	DMSO-d_6 $\epsilon = 46.7$
10^3k_{obs} (**1f**)	7.92 ± 0.2	20.8 ± 0.9	24.5 ± 0.3
N/X (**1f**)	12.7 ± 0.5	≥19.0[c]	≥19.0[c]
10^3k_{obs} (**1g**)	12.7 ± 0.3	7.65 ± 0.3	12.8 ± 0.3
N/X (**1g**)	8.7 ± 0.6	7.0 ± 0.7	8.7 ± 0.6

[a] Second order rate constants (L/mol s) and endo/exo ratios obtained from kinetic runs over 30 min at 60 °C. $[fulvene]_o = [maleimide]_o = 0.0667$ M. Standard error of the rate constant from least-squares regression. [b] Standard deviation of the average ratio over the run. [c] Actual concentration of exo adduct could not be determined due to signal-to-noise ratio complications when present at ≤5%.

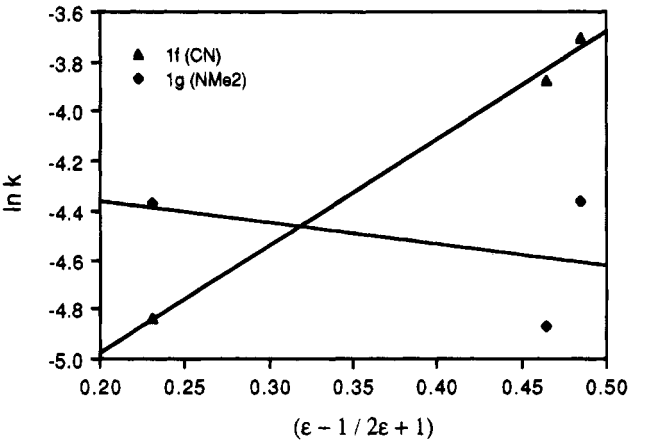

Figure 4. Plot of ln k versus Kirkwood function for **1f** and **1g** at 60 °C. Straight lines are from the least-squares regression: ln k (**1f**) = −5.840 + 4.32x, r = 1.00; ln k (**1g**) = −4.184 − 0.880x, r = 0.43.

One must also consider that for steric reasons, the phenyl and fulvene π-subsystems are not completely coplanar and thus π-electronic transmission through resonance would be attenuated by the twist. The resonance effect is expected to drop off by $\cos^2\theta$, where θ is the twist angle between the π-subsystems.[15] If the twist angle is independent of the electronic character of the para substituent, there should be a constant steric environment presented to the incoming dienophile and any variation in the endo/exo selectivity should be a result of electronic consequences.

However, steric interactions between the aryl ring and the dienophile would be more pronounced in the exo Diels–Alder transition state (Chart 1). If the twist angle is influenced by the nature of the para substituent, we would expect the extent of coplanarity to be greatest with strong donor substituents due to the compensation of

(15) Hamer, G. K.; Peat, I. R.; Reynolds, W. F. *Can. J. Chem.* **1973**, *51*, 915–926.

Chart 1

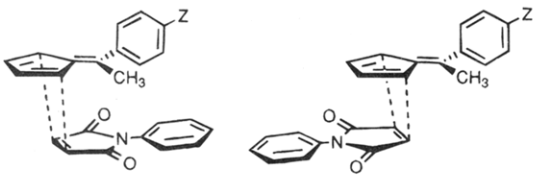

steric strain by aromatic resonance contributions. Conversely, strong acceptor substituents should induce the largest twist angles. Thus the differences in endo/exo selectivity could be a result of the varying steric environment as influenced by the substituent. We turned to molecular orbital calculations to help clarify the situation.

Molecular Orbital Calculations. Previous computations of electronic structure of 6-arylfulvenes have typically assumed a twist angle between the π-subsystems that remains constant regardless of substituent with limited (if any) minimization of the standard geometry.[6a,7b] One notable exception is a recent comparison of crystal structure with RHF/STO-3G optimized geometry for 6-(*p*-(dimethylamino)phenyl)fulvene.[1a] It seems important to examine the possibility that the twist angle may be substituent dependent and therefore we carried out full geometry optimizations on fulvenes **1a**–**1i** utilizing the density functional program DMOL.[16] Structures were optimized without symmetry constraints using gradient optimizations with the local density approximation, JMW functionals, and a double numeric plus polarization basis set. Population analyses on the optimized structures were performed using a 3-21G* basis set and the natural bond orbital (NBO) method contained in the Gaussian 92 program.[17] The optimized structures of **1a** and **1g** are shown in Figures 5 and 6.

Substituent-induced changes in geometry were relatively minor except for the *p*-NMe_2 substituted fulvene (see Table 5). A decrease in the preferred twist angle from 54–55° (seen in all other examples) to 36° reflects the better donating ability of the NMe_2 group.[18] This decrease is accompanied by a twisting of the substituents on the exocyclic fulvene carbon out of the fulvene plane and a substantial change in the C6–C1 and C6–C8 bond lengths. At a 36° twist angle, the contact distances between ortho-H's on the phenyl ring and hydrogens on C2 and C7 are already 0.1 Å less than the sum of the van der Waals radii ($\sum r_{vdw}$ = 2.4 Å).[19] This value may be the lower limit for coplanarity in the gas phase, which is considerably higher in comparison to the solid state twist angle found for 6-(*p*-(dimethylamino)phenyl)fulvene of 15°.[1a] The 36° conformation was further investigated for **1a** (Z = H), **1c** (Z = OMe), and **1f** (Z = CN). After geometry optimization, it was found to be 1.7, 0.97, and 2.2 kcal/mol, respectively, less stable than the global minimum at 54°. These results lend support to the idea that the extent of overlap of the phenyl and fulvene

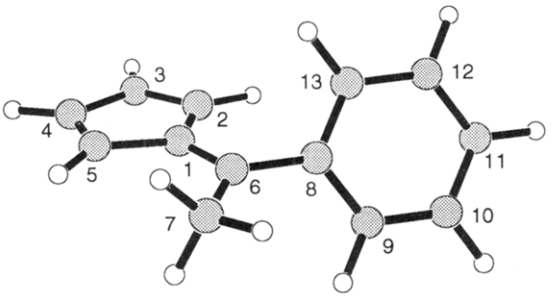

Figure 5. Optimized geometry of 6-phenyl-6-methylvulvene (**1a**).

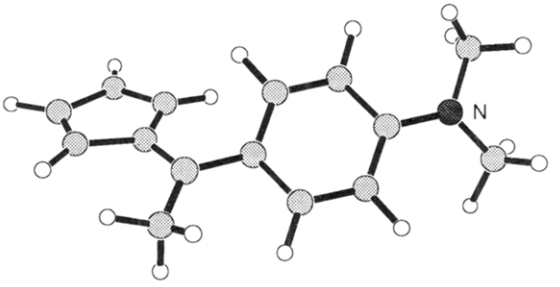

Figure 6. Optimized geometry of 6-(*p*-(dimethylamino)phenyl)-6-methylfulvene (**1g**).

subsystems is increased by electron-releasing substituents and that the degree of compensation by conjugation with the fulvene system to the energy expenditure due to unfavorable conformation depends on the electronic character of the substituent.

Variation of the para substituent also caused subtle changes in the electron distribution of the fulvene ring. Tables 6 and 7 list the calculated π-charge densities and NBO atomic charge densities, respectively. The electron density at the exocyclic carbon C6 was most sensitive to a change in electronic nature of the substituent. As the electron acceptor ability of the substituent increases, the electron density at C6 increases (becomes less positive) which is characteristic of an inverse substituent effect operating at this position. Normal substituent effects are seen at C1, C3, and C4 where increasing acceptor ability of the substituent causes a decrease in electron density. There are no simple electronic trends found for the substituent effects on the charge densities at C2 and C5.

On the basis of the Arrhenius form of the rate constant, we would expect a linear relationship between ln k and a molecular property of the fulvenes that affects the energy of the corresponding TS. With regard to the calculated π-charges, the observed rate roughly increases with increasing π-charge at C1, C3, and C4 while it decreases with increasing π-charge at C2, C5, and C6. More notable, there is a fair quantitative correlation (Figure 7) between the dipole moment and the observed rate (e.g., an increase in dipole moment produces a decrease in rate) as well as a reasonable trend in the kinetic endo selectivity as a response to the direction of the molecular dipole vector.

On the basis of the RHF/3-21G* calculations, the fulvenes can be divided into two groups: (1) where the negative end of the dipole points toward the fulvene portion and (2) where it points toward the phenyl ring (Figure 8). The dipole moment of the dienophile lies along the symmetry axis with the positive end toward the maleimide C=C bond. Expecting the direction of the reactant dipoles to remain approximately the same in the

(16) DMOL, Version 2.3, Biosym Technologies, Inc., San Diego, CA, 1993.

(17) (a) Gaussian 92, Revision E.2. Frisch, M. J.; Trucks, G. W.; Head-Gordon, M.; Gill, P. M. W.; Wong, M. W.; Foresman, J. B.; Johnson, B. G.; Schlegel, H. B.; Robb, M. A.; Replogle, E. S.; Gomperts, R.; Andres, J. L.; Raghavachari, K.; Binkley, J. S.; Gonzalez, C.; Martin, R. L.; Fox, D. J.; Defrees, D. J.; Baker, J.; Stewart, J. J. P.; Pople, J. A., Gaussian, Inc., Pittsburgh PA, 1992. (b) NBO, Version 3.1. Glendening, E. D.; Reed, A. E.; Carpenter, J. E.; Weinhold, F.

(18) This value compares very well to that calculated for 6-(*p*-(dimethylamino)phenyl)fulvene (35°) in spite of the additional steric interactions due to the exocyclic methyl group in our system.

(19) Pauling, L. *The Nature of the Chemical Bond*, 3rd ed.; Cornell University Press: Ithaca, NY, 1960; p 260.

Table 5. Selected Geometrical Parameters from Optimized Structures

parameter[a]	NMe_2	OMe	F	Cl	Me	CF_3	CN	NO_2	H	AVE	SD
					Distances (Å)						
1–5	1.448	1.450	1.449	1.450	1.451	1.450	1.452	1.451	1.450	1.448	0.001
1–2	1.455	1.456	1.457	1.457	1.458	1.458	1.457	1.458	1.457	1.457	0.001
2–3	1.364	1.360	1.361	1.360	1.361	1.359	1.358	1.359	1.361	1.360	0.002
4–5	1.366	1.362	1.362	1.362	1.363	1.361	1.360	1.361	1.361	1.362	0.002
3–4	1.448	1.453	1.456	1.454	1.455	1.456	1.455	1.458	1.455	1.454	0.003
1–6	1.373	1.362	1.361	1.361	1.363	1.360	1.361	1.361	1.361	1.363	0.004
6–7	1.490	1.491	1.491	1.491	1.492	1.491	1.492	1.491	1.492	1.491	0.001
6–8	1.445	1.460	1.460	1.458	1.460	1.461	1.461	1.458	1.460	1.458	0.005
ArC=C[b]	1.397	1.392	1.389	1.391	1.393	1.391	1.394	1.389	1.392	1.392	0.002
H2–H9	2.304	2.543	2.545	2.536	2.545	2.541	2.488	2.534	2.552	2.510	0.079
H7–H13	2.305	2.565	2.574	2.565	2.577	2.568	2.579	2.492	2.597	2.536	0.091
					Angles (deg)						
1–6–7	121.1	121.9	122.1	122.4	122.0	122.2	122.0	122.4	122.1	122.0	0.4
1–6–8	121.4	121.2	120.7	120.6	120.9	120.8	120.8	120.7	121.1	120.9	0.3
8–6–7	117.5	116.7	117.2	117.0	117.1	117.0	117.2	117.0	116.9	117.1	0.2
5–1–6–7	12.5	1.5	1.0	1.4	1.6	1.5	1.7	2.5	1.5	2.8	4
2–1–6–7	−164	−176	−176	−176	−176	−176	−175	−175	−176	−174	4
5–1–6–8	−170	−178	−179	−179	−179	−179	−179	−179	−178	−178	3
2–1–6–8	13.8	4.5	4.0	4.2	3.7	3.8	5.0	3.5	4.0	5.2	4
θ[c]	36.0	54.1	54.0	54.1	54.2	54.5	53.8	54.7	55.1	52.3	6

[a] The numbering scheme is given in Figure 5. Unless otherwise noted, interactions pertain to the carbon skeleton. [b] The average of all carbon–carbon bond distances in the substituted phenyl ring. [c] The twist angle between π-subsystems is defined as the dihedral angle 1–6–8–13.

Table 6. RHF/3-21G* NBO π-Charges of Fulvene Moiety and Dipole Moments

Z	q_1	q_2	q_3	q_4	q_5	q_6	μ (D) calcd	μ (D)[a] expl
NMe_2	−0.0770	−0.0637	−0.0617	−0.0276	−0.0799	0.1577	4.28	(2.75)[b]
OMe[c]	−0.0576	−0.0678	−0.0465	−0.0190	−0.0831	0.1411	3.24	1.90
Me	−0.0525	−0.0378	−0.0409	−0.0113	−0.0650	0.1342	2.23	1.34
H	−0.0473	−0.0370	−0.0390	−0.0096	−0.0653	0.1275	1.86	1.19
F	−0.0454	−0.0426	−0.0353	−0.0076	−0.0658	0.1239	1.83	
Cl	−0.0416	−0.0415	−0.0336	−0.0060	−0.0649	0.1206	1.87	
CF_3	−0.0346	−0.0427	−0.0288	−0.0017	−0.0650	0.1113	3.21	
CN	−0.0330	−0.0453	−0.0303	−0.0006	−0.0692	0.1085	4.22	
NO_2	−0.0300	−0.0456	−0.0310	0.0004	−0.0716	0.0950	5.08	
OMe[d]	−0.0518	−0.0374	−0.0336	−0.0113	−0.0577	0.1377	1.96	1.90

[a] Determined in benzene at 20 °C. See ref 4a. [b] 6-(*p*-Piperidinylphenyl)-6-methylfulvene. [c] Twist angle of 36.4°. [d] Twist angle of 54.1°.

Table 7. RHF/3-21G* Total NBO Atomic Charges of Fulvene Moiety

Z	q_1	q_2	q_3	q_4	q_5	q_6	θ
NMe_2	−0.1424	−0.2573	−0.2722	−0.2596	−0.2591	0.1380	36.0
OMe	−0.1240	−0.2578	−0.2650	−0.2507	−0.2606	0.1195	36.4
Me	−0.1239	−0.2459	−0.2682	−0.2473	−0.2620	0.1169	54.2
H	−0.1197	−0.2458	−0.2666	−0.2452	−0.2615	0.1116	55.1
F	−0.1177	−0.2501	−0.2630	−0.2439	−0.2623	0.1089	54.0
Cl	−0.1142	−0.2502	−0.2619	−0.2428	−0.2623	0.1043	54.1
CF_3	−0.1072	−0.2520	−0.2581	−0.2394	−0.2635	0.0950	54.5
CN	−0.1049	−0.2531	−0.2571	−0.2380	−0.2642	0.0922	53.8
NO_2	−0.0990	−0.2545	−0.2538	0.2361	−0.2646	0.0847	54.7
OMe	−0.1247	−0.2470	−0.2668	−0.2474	−0.2614	0.1182	54.1

TS, the exo TS would have a greater net moment for group 2 whereas the endo TS would have a larger moment for group 1. This electrostatic effect does appear to be reflected in the kinetic stereoselectivity data, especially for fulvenes having strong dipole moments.

At this point, it becomes intriguing to question if the substituent effect on frontier MO's of the fulvene moiety provides a rationale for the observed Diels–Alder behavior. Tables 8 and 9 and Figure 9 give the RHF/3-21G* calculated eigenvectors and eigenvalues for the two highest occupied π and lowest unoccupied π MO's of the fulvenes. Using the local symmetry of the fulvene moiety, the HOMO is an antisymmetric orbital (a_2), while the NHOMO and LUMO are symmetric orbitals (b_1). As expected, electron-withdrawing substituents lower the energies of the NHOMO, HOMO, and LUMO.

The HOMO and NHOMO energies are nicely correlated with Hammett σ values ($\varrho = -0.027$, $r = 0.99$, $\psi = 0.1$ and $\varrho = -0.037$, $r = 0.97$, $\psi = 0.3$, respectively), and a fair LFER exists between LUMO energies and σ^- values ($\varrho = -0.020$, $r = 0.92$, $\psi = 0.4$). Strong electron-

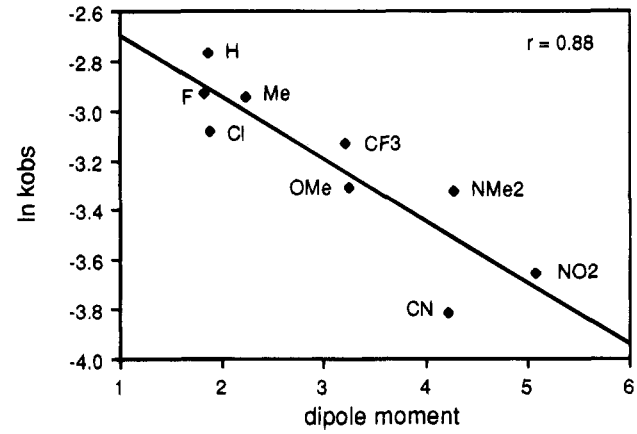

Figure 7. Plot of reactivity versus calculated dipole moment of fulvene.

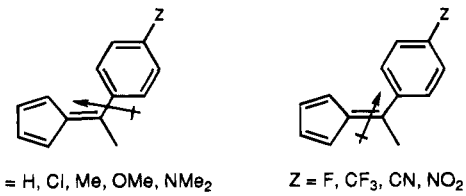

Figure 8. Schematic diagram of the calculated direction of the molecular dipole moments.

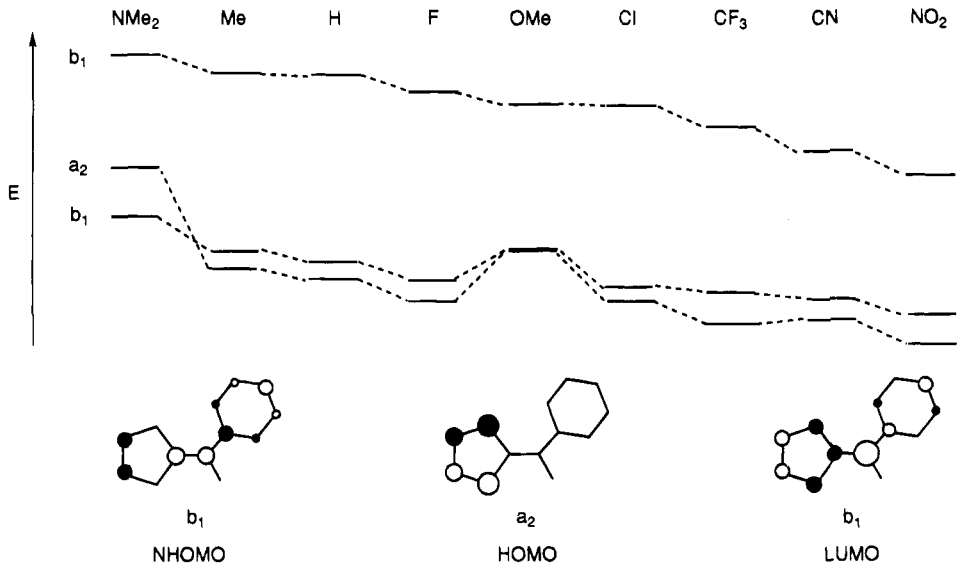

Figure 9. Frontier orbital energies of substituted 6-phenyl-6-methylfulvenes.

Table 8. RHF/3-21G* Eigenvalues and Eigenvectors for NHOMO and HOMO π Orbitals of *p*-Substituted Phenylmethylfulvenes

Z	*E* (au)	C_1	C_2	C_3	C_4	C_5	C_6
			NHOMO (b_1)				
NMe_2	−0.262[a]	0.420	0.037	−0.245	−0.282	−0.020	0.259
OMe[b]	−0.292	0.487	−0.140	−0.413	−0.229	0.106	0.404
Me	−0.298	0.484	−0.078	−0.358	−0.302	−0.004	0.431
H	−0.304	0.502	−0.056	−0.357	−0.342	−0.046	0.473
F	−0.309	0.499	−0.063	−0.356	−0.336	−0.042	0.467
Cl	−0.309	0.487	−0.066	−0.350	−0.324	−0.035	0.456
CF_3	−0.320	0.519	−0.074	−0.373	−0.360	−0.061	0.519
CN	−0.319	0.495	−0.065	−0.352	−0.333	−0.050	0.483
NO_2	−0.327	0.506	−0.074	−0.368	−0.354	−0.067	0.525
			HOMO (a_2)				
NMe_2	−0.281[a]	0.018	−0.572	−0.421	0.395	0.595	0.003
OMe	−0.292	−0.110	−0.553	−0.329	0.469	0.582	−0.098
Me	−0.292	−0.029	−0.600	−0.419	0.442	0.617	−0.028
H	−0.294	−0.007	−0.599	−0.434	0.425	0.617	−0.007
F	−0.299	−0.009	−0.602	−0.429	0.431	0.616	−0.011
Cl	−0.300	−0.013	−0.602	−0.428	0.433	0.619	−0.014
CF_3	−0.305	−0.006	−0.604	−0.431	0.429	0.619	−0.009
CN	−0.307	−0.005	−0.599	−0.427	0.426	0.612	−0.009
NO_2	−0.311	−0.005	−0.592	−0.422	0.420	0.606	−0.008

[a] Due to crossover in a_2 and b_1 levels with this substituent, the b_1 orbital becomes the HOMO and a_2 the NHOMO. [b] Twist angle of 36.4°.

Table 9. RHF/3-21G* Eigenvalues and Eigenvectors for LUMO π Orbitals of *p*-Substituted Phenylmethylfulvenes

Z	*E* (au)	C_1	C_2	C_3	C_4	C_5	C_6
			LUMO (b_1)				
NMe_2	0.066	−0.320	−0.321	0.328	0.376	−0.354	0.709
OMe	0.055	−0.345	−0.311	0.334	0.378	−0.339	0.683
Me	0.064	−0.333	−0.394	0.367	0.421	−0.402	0.710
H	0.063	−0.336	−0.395	0.371	0.422	−0.405	0.710
F	0.057	−0.341	−0.394	0.373	0.425	−0.403	0.713
Cl	0.054	−0.345	−0.382	0.365	0.418	−0.391	0.692
CF_3	0.046	−0.350	−0.364	0.353	0.407	−0.371	0.657
CN	0.039	−0.344	−0.324	0.323	0.378	−0.331	0.597
NO_2	0.024	−0.277	−0.228	0.238	0.287	−0.234	0.425

releasing substituents destabilize the NHOMO orbital to a large extent (and the HOMO to a lesser degree) such that the calculations predict a degeneracy of the HOMO and NHOMO for *p*-OMe and a crossover in these levels for *p*-NMe_2. For a normal electron demand Diels–Alder reaction one would expect charge donation from the fulvene HOMO to the dienophile LUMO to be the dominant interaction and therefore a reduction in rate with decreasing HOMO energy of the fulvene. Excluding the irregular NMe_2 and OMe examples, there is a qualitative agreement in this sense between calculated HOMO energies and reactivity.

Conclusions. The experimental and theoretical results of this study clearly suggest an important contribution of dipolar resonance forms to the observed behavior of the *p*-phenyl-substituted fulvene molecule, particularly at the donor/acceptor substituent extremes. Nevertheless, one must conclude that the response of these fulvenes in their reaction with *N*-phenylmaleimide ultimately arises from a subtle interplay among electronic, steric, and electrostatic influences that vary with the nature of each substituent.

Experimental Section

General. All commercially available precursors were obtained from Aldrich and used without further purification. ^1H NMR spectra for kinetic runs in C_6D_6 were recorded on a 250 MHz FT-NMR with a variable temperature probe rated at ±1 °C unless otherwise noted. All other ^1H NMR spectra were recorded in $CDCl_3$ at 200, 250, or 500 MHz. ^{13}C NMR were recorded in $CDCl_3$ at 50 or 62.9 MHz as indicated. IR spectra were recorded on a FT-IR spectrometer in $CHCl_3$ solution. Melting points are uncorrected. Elemental analyses were obtained from M-H-W Laboratories, Phoenix, AZ. Exact mass determinations were obtained at the University of Guelph Mass Spectrometry Centre. Solvents were reagent grade and dried prior to use. All reactions were conducted under a nitrogen atmosphere. Fulvenes **1a–f** were prepared according to literature procedures.[6a] The instability of these compounds towards oxidation and dimerization precluded obtaining elemental analyses of the new fulvenes **1g–j** which were characterized by their spectral data.

6-(*p*-(Dimethylamino)phenyl)-6-methylfulvene (1g). To a cold solution of potassium hydroxide (2.87 g, 51 mmol) in methanol (28 mL) was added a methanol solution containing *p*-(dimethylamino)acetophenone[20] (3.82 g, 23 mmol) and freshly distilled cyclopentadiene (1.95 mL, 24 mmol) dropwise via an addition funnel. The reaction mixture was warmed to rt and stirred overnight. The mixture was diluted with water (100 mL) and extracted with CH_2Cl_2 (3 × 200 mL). The extracts were dried over anhyd Na_2SO_4 and concentrated under reduced pressure. Purification of the dark orange oil by chromatography on silica gel (elution with 20% diethyl ether in

(20) Lienhard, U.; Fahrni, H.-P.; Neuenschwander, M. *Helv. Chim. Acta* **1978**, *61*, 1609–1621.

hexanes) provided 0.56 g (12%) of the fulvene as an orange oil that slowly solidifies upon standing: IR (cm^{-1}) 3003, 1598, 1523, 1363, 1216, 799, 742; ^1H NMR (250 MHz) δ 7.36 (d, J = 8.6 Hz, 2 H), 6.69 (d, J = 8.6 Hz, 2 H), 6.58–6.65 (m, 1 H), 6.45–6.55 (m, 2 H), 6.33–6.40 (m, 1 H), 2.98 (s, 6H), 2.53 (s, 3 H); ^{13}C NMR (62.5 MHz) ppm 161.1, 150.6, 141.6, 131.2, 130.3, 130.1, 129.5, 123.7, 120.9, 111.3, 40.1, 22.1.

6-(*p*-Nitrophenyl)-6-methylfulvene (1i). To an ice-cooled solution of sodium metal (0.2 g, 8.7 mmol) in anhyd methanol (25 mL) was added freshly distilled cyclopentadiene (0.6 g, 9 mmol). *p*-Nitroacetophenone (1.25 g, 7.5 mmol) in methanol was then added dropwise. The reaction mixture was allowed to warm to room temperature and stirred for 2 h. After neutralization with 1 N HCl, the solvent was removed *in vacuo*. The residue was dissolved in ether (100 mL) and washed with water (25 mL) and brine (25 mL). The organic phase was then dried over anhyd $MgSO_4$ and the solvent removed under reduced pressure. Purification of the crude product by chromatography on silica gel (elution with hexanes: Et_2O = 1:1) afforded 0.88 g (55%) of the fulvene as a viscous, red oil: IR (cm^{-1}) 3018, 1594, 1518, 1347, 1219, 859, 775; ^1H NMR (250 MHz) δ 8.22 (d, J = 8.9 Hz, 2 H), 7.52 (d, J = 8.9 Hz, 2 H), 6.58–6.63 (m, 2 H), 6.45–6.51 (m, 1 H), 6.01–6.05 (m, 1 H), 2.55 (s, 3 H); ^{13}C NMR (62.5 MHz) ppm 148.4, 148.3, 145.8, 144.9, 133.1, 132.9, 129.8, 123.0, 122.7, 121.1, 22.1.

6-(*p*-(Trifluoromethyl)phenyl)-6-methylfulvene (1h). To a suspension of NaH (50% in oil, 0.25 g, 5 mmol) in anhyd THF (20 mL) at 0 °C was added slowly freshly distilled cyclopentadiene (0.4 g, 6 mmol) in THF (10 mL). The light pink solution was stirred for 10 min, and then *p*-(trifluoromethyl)acetophenone (0.94 g, 5 mmol) in THF (10 mL) was added slowly. The reaction mixture was warmed to rt and stirred for 30 min. After dilution with diethyl ether (150 mL), the reaction was quenched with saturated NH_4Cl solution. The organic phase was washed with water (30 mL) and brine (30 mL) and then dried over anhyd $MgSO_4$. Concentration under reduced pressure followed by purification of the crude product by chromatography on silica gel (elution with hexanes:Et_2O = 7:3) gave 0.87 g (74%) of the fulvene as a viscous, red oil: IR (cm^{-1}) 3008, 1616, 1326, 1213, 1131, 845, 789; ^1H NMR (250 MHz) δ 7.63 (d, J = 8.5 Hz, 2 H), 7.46 (d, J = 8.5 Hz, 2 H), 6.55–6.65 (m, 2 H), 6.40–6.50 (m, 1 H), 6.02–6.10 (m, 1 H), 2.53 (s, 3H); ^{13}C NMR (62.5 MHz) ppm 147.5, 145.6, 144.4, 143.1, 132.7, 132.4, 129.4, 124.9, 123.2 (q, J_{CF} = 270 Hz), 121.1, 116.1, 22.4.

6-(*p*-(*N*-Acetyl-*N*-methylamino)phenyl)-6-methylfulvene (1j). To a suspension of NaH (50% in oil, 0.19 g) in anhyd THF (40 mL) was added freshly distilled cyclopentadiene (0.26 g, 4.0 mmol). The mixture was stirred at rt for 15 min followed by addition of *p*-(*N*-acetyl-*N*-methylamino)-acetophenone (0.68 g, 3.6 mmol) in anhyd THF (10 mL). The reaction mixture was stirred at rt for 24 h and then quenched using saturated NH_4Cl. Diethyl ether (150 mL) was added, and the organic phase was washed with water and then brine and dried over anhyd $MgSO_4$. The solvent was removed under reduced pressure to give a brown solid. Purification of the residue by chromatography on silica gel (elution with Et_2O: hexanes = 1:1) afforded 360 mg (42%) of the fulvene as a yellow solid: mp 104–105.5 °C; IR (cm^{-1}) 3005, 1645, 1508, 1376, 1220, 785, 739; ^1H NMR (250 MHz) δ 7.43 (d, J = 8.3 Hz, 2 H), 7.22 (d, J = 8.3 Hz, 2 H), 6.4–6.7 (m, 3 H), 6.1–6.2 (m, 1 H), 3.30 (s, 3 H), 2.55 (s, 3 H), 1.94 (s, 3 H); ^{13}C NMR (62.5 MHz) ppm 170.1, 147.8, 144.1, 143.6, 141.0, 131.9, 131.8, 130.2, 128.2, 123.0, 120.9, 36.9, 22.3 (2 C).

Prototypical Cycloaddition of 1 with *N*-Phenylmaleimide. For characterization of the products, scaled up reactions were carried out in refluxing toluene where the endo/exo ratios were generally between 3:1 and 1:1. A mixture of 1 (0.25 mmol) and *N*-phenylmaleimide (0.25 mmol) in toluene (5 mL) was heated to reflux under nitrogen for 2 days. Concentration of the reaction mixture, followed by chromatography on silica gel (elution with Et_2O:CH_2Cl_2:hexanes = 1:2:2), allowed for isolation of the individual adducts. Full characterizations of the individual isomers are given in the supplementary material.

Kinetics. Rate constants for the reaction of **1** with *N*-phenylmaleimide in C_6D_6 were determined at the indicated temperature in the NMR. NMR tubes containing solutions of **1** (0.05 mmol) in C_6D_6 (0.5 mL) were heated in the probe of the machine. The tube was removed, and *N*-phenylmaleimide (0.05 mmol) in C_6D_6 (0.25 mL) was added. The tube was returned to the probe and shimmed to constant values (ca. 1 min). Data (16 scans) were collected at 5 min time intervals over 1 h. Relative concentrations of **1**, the endo adduct (**2**), and the exo adduct (**3**) were determined by comparison of the integrations of the 6-Me protons in **1**, **2**, and **3**, normalized to 100%. A precise measurement of the exo adduct **3** was impossible when present at less than 5% of the reaction mixture due to the signal-to-noise ratio. The absolute error in the observed ratios was estimated by comparison of known ratios from carefully prepared mixtures of endo/exo isomers to that obtained by ^1H NMR integration of the mixtures. Ratios from integration were consistently 7% low throughout the series. In the case of **1j**, a 500 MHz NMR was utilized to achieve adequate resolution of the diagnostic signals.

Second-order rate constants were obtained by linear regression from slopes of plots of 1/[fulvene] vs time. These plots were linear over ca. 5 half-lives (r > 0.99) after which severe curvature occurred in several cases. Variable temperature studies (30–80 °C) were carried out for **1a**, **1f**, and **1g**. Linear Arrhenius and Eyring plots (r > 0.99) were obtained for these reactions. Activation parameters were determined from least-squares analyses of ln k and ln (k/T) vs $1/T$ plots.

Solvent Studies. Rate constants for the Diels–Alder reaction of **1a**, **1f**, and **1g** were determined at 60 °C in acetone-d_6 and DMSO-d_6 following the same procedure given above. In the case of **1f**, the relative concentrations of starting material to endo and exo adduct were determined by comparison of the integrations of the vinylic protons in *N*-phenyl maleimide and the bridgehead protons in **2** and **3**, normalized to 100%.

Equilibrium Studies. The equilibrium composition of endo/exo adducts were determined in C_6D_6 at 80 °C. For this, NMR tubes containing solutions of **1** (0.05 mmol) and *N*-phenylmaleimide (0.05 mmol) in C_6D_6 (0.75 mL) were heated in a bath of refluxing benzene. The reaction mixtures were monitored by ^1H NMR at various time intervals up to 120 h. Equilibrium was slowly established over an extended reaction time of 96 h after which there was no significant changes seen in the product ratios.

Acknowledgment. We are grateful to the Natural Sciences and Engineering Research Council (NSERC) Canada for financial support. We also thank Scott Paterson and Brian Go for their assistance in the early stages of this work.

Supplementary Material Available: Copies of ^1H NMR spectra for new fulvenes **1g–j** and full characterizations (spectral and analytical data) for compounds **2** and **3** (9 pages). This material is contained in libraries on microfiche, immediately follows this article in the microfilm version of the journal, and can be ordered from the ACS; see any current masthead for ordering information.